Determination of Global Protein Turnover in Stressed Mycobacterium Cells Using Hybrid-Linear Ion Trap-Fourier Transform Mass Spectrometry

ARTICLE *in* ANALYTICAL CHEMISTRY · JANUARY 2008

Impact Factor: 5.64 · DOI: 10.1021/ac701690d · Source: PubMed

3 AUTHORS, INCLUDING:

Bryan Roxas
The University of Arizona
21 PUBLICATIONS **346** CITATIONS

SEE PROFILE

Anal. Chem. **2008,** *80,* 396−406

Determination of Global Protein Turnover in Stressed Mycobacterium Cells Using Hybrid-Linear Ion Trap-Fourier Transform Mass Spectrometry

Prahlad K. Rao,[†] Bryan A. P. Roxas,[†] and Qingbo Li*[,†,‡]

Center for Pharmaceutical Biotechnology and Department of Microbiology and Immunology, University of Illinois at Chicago, Chicago, Illinois 60607

We determined the global protein turnover profiles for *Mycobacterium smegmatis* under acid shock and iron starvation conditions using a simple ^{15}N isotope doping technique and a complete medium replacement method for chasing. We used a high-resolution hybrid-linear ion trap-Fourier transform mass spectrometer coupled with nanoliquid chromatography separation to measure protein turnover values for 151 proteins over a dynamic range of 3 orders of magnitude ranging from about 0.2 to 500. Of these 151 proteins, 31 had significant protein turnover changes (p <0.05) at both stress conditions and had protein turnover values increased or decreased by more than 2-fold under at least one stress condition. Protein turnover increased under acid shock for 28 of the 31 proteins but decreased under iron starvation for all the 31 proteins. Only two proteins had protein turnover lowered by more than 2-fold (p <0.05) under both stress conditions, including an ATP synthase F1 β subunit (MSMEG4921; AtpD) and a catalase/peroxidase (MSMEG6346; KatG). KatG is required for in vivo activation of isoniazid to be bacterialcidal. Decrease of KatG protein turnover under both stress conditions supports the view that isoniazid may induce a dormancy program in mycobacteria, which in turn limits the efficacy of this drug against dormant subpopulation of mycobacteria. Thus, measuring protein turnover in stressed Mycobacterium cells has implications in understanding drug action and resistance mechanisms.

Steady-state protein abundance in an organism is the result of a delicate balance between de novo synthesis and degradation, which is governed by the cell's dynamic regulation machinery in response to the ever-changing environment. It has been well acknowledged that intracellular protein degradation and turnover is a fundamental process in all cell types and has important implications to biochemical regulations, genetics, physiology, and medicine.[1,2] While many comparative proteomic studies have been providing relative abundance information of proteins in an organism under different perturbations, few have yet comprehensively explored protein turnover at a global level.[3] It has been noted that an increase in protein abundance does not always result from de novo protein synthesis. Rather, it can be the consequence of protein degradation inhibition imposed by a cellular signaling process or a side effect of drug treatment.[4] The ability to determine protein turnover in addition to relative abundance will therefore provide a view of the dynamic nature of a proteome.[3] In this work, we adopt the definition of protein turnover as the synthesis over degradation ratio (S/D) calculated as the relative abundance of de novo synthesized and old proteins in a ^{13}C stable isotope chasing experiment demonstrated by Cargile et al.[5]

Earlier work on protein turnover measurements relied on a radioactive isotope for metabolic labeling.[1] With the advent of mass spectrometry capable of accurate measurement of peptides and proteins, recent studies on protein synthesis, degradation, and turnover dynamics have more frequently used stable isotopes such as ^{2}H or ^{13}C in the form of amino acids or carbon source for chasing and used MALDI mass spectrometry to determine the identity and the relative abundance of old and de novo synthesized proteins.[3,5−8] Although both MALDI-MS and LCQ-MS were used by Cargile et al.,[5] the ultimate measurement of isotopomer profiles was done with MALDI-MS, probably due to the need for better mass accuracy and resolution offered by MALDI-MS. None of these works, however, demonstrated automation in both the mass spectrometry analysis step and the data processing step suitable for large-scale determination of protein turnover. In the work reported here, we utilized the high-resolution, high mass accuracy hybrid-linear ion trap-Fourier transform mass spectrometry (LTQ-FT) in combination with a data processing algorithm from previous large-scale quantitative proteomic studies[9,10] for protein turnover

* To whom correspondence should be addressed. E-mail: qkli@uic.edu. Phone: 312-413-9301. Fax: 312-413-9303.

[†] Center for Pharmaceutical Biotechnology.

[‡] Department of Microbiology and Immunology.

(1) Larrabee, K. L.; Phillips, J. O.; Williams, G. J.; Larrabee, A. R. *J. Biol. Chem.* **1980**, *255*, 4125−4130.

(2) Wilkinson, K. D. *Proc. Natl. Acad. Sci. U.S.A.* **2005**, *102*, 15280−15282.

(3) Pratt, J. M.; Petty, J.; Riba-Garcia, I.; Robertson, D. H.; Gaskell, S. J.; Oliver, S. G.; Beynon, R. J. *Mol. Cell. Proteomics* **2002**, *1*, 579−591.

(4) Wu, C. C.; MacCoss, M. J.; Howell, K. E.; Matthews, D. E.; Yates, J. R., 3rd. *Anal. Chem.* **2004**, *76*, 4951−4959.

(5) Cargile, B. J.; Bundy, J. L.; Grunden, A. M.; Stephenson, J. L., Jr. *Anal. Chem.* **2004**, *76*, 86−97.

(6) Doherty, M. K.; Whitehead, C.; McCormack, H.; Gaskell, S. J.; Beynon, R. J. *Proteomics* **2005**, *5*, 522−533.

(7) Bouwman, F.; Renes, J.; Mariman, E. *Proteomics* **2004**, *4*, 3855−3863.

(8) Vogt, J. A.; Hunzinger, C.; Schroer, K.; Holzer, K.; Bauer, A.; Schrattenholz, A.; Cahill, M. A.; Schillo, S.; Schwall, G.; Stegmann, W.; Albuszies, G. *Anal. Chem.* **2005**, *77*, 2034−2042.

(9) Andreev, V. P.; Li, L.; Rejtar, T.; Li, Q.; Ferry, J. G.; Karger, B. L. *J. Proteome Res.* **2006**, *5*, 2039−2045.

10.1021/ac701690d CCC: $40.75
Published on Web 12/18/2007

measurements. The process we demonstrate here is amendable to measurement of protein turnover at a large scale with automation to an extent similar to that established for genome-wide relative protein abundance measurements.[11,12]

In this work, we used the biological model of Mycobacterium cells under acid shock and iron starvation for studying protein turnover. *Mycobacterium tuberculosis* has been a difficult problem in biomedical endeavors. It is an extremely successful intracellular pathogen residing within human macrophages that are essential in host defense against pathogen invasion. Upon phagocytosis, macrophages typically expose microbes to reactive oxidative species (ROS), lytic enzymes, acid, nutrient limitation, low oxygen, and other stresses typically present in a stationary-phase culture.[13] *M. tuberculosis*, however, is remarkably capable of resisting these stresses, surviving and even replicating within macrophages.[14] During the latency of tuberculosis disease, *M. tuberculosis* is believed to enter a dormant state at which the bacilli are highly resistant to antibiotics. Studying protein turnover dynamics in Mycobacterium cells under stresses thus bears biological and therapeutic significance. Since *Mycobacterium smegmatis* is a fast-growing, nonpathogenic Mycobacterium widely used as a model system, we used *M. smegmatis* strain mc^2 155 as a surrogate organism in this work. We used [^{15}N]/[^{14}N] metabolic labeling to chase cells upon exposure to acid shock or iron starvation and performed proteomic analysis on a nanoLC/LTQ-FT system to determine global protein turnover profiles of *M. smegmatis* under the two stress conditions. Biological implication of the protein turnover measurements is discussed.

MATERIALS AND METHODS

Chemicals, Media, and Bacterial Strain. Dextrose, Tween 80, citric acid, biotin, pyridoxine, NaCl, Na_2HPO_4, KH_2PO_4, $MgSO_4 \cdot 6H_2O$, $CuSO_4 \cdot 5H_2O$, $ZnSO_4 \cdot 6H_2O$, $CaCl_2 \cdot 2H_2O$, ferric ammonium citrate, ammonium bicarbonate, and acetonitrile were purchased at certified ACS or reagent grade from Fisher Scientific (Pittsburgh, PA). 7H9 broth base and 99At%[^{15}N]ammonium sulfate were purchased from Sigma (St. Louis, MO). At% denotes atomic percent. Sequencing grade trysin was obtained from Promega (Madison, WI). *M. smegmatis* strain mc^2 155 was obtained from the American Type Culture Collection (ATCC; Rockville, Md).

Cell Culturing, Metabolic Labeling, and Sample Preparation. Two stable isotope labeling approaches were taken to suit two different experimental settings (Figure 1). In the acid shock experiment in which complete medium replacement was not required, we used an isotope doping technique to generate 50At%-[^{15}N] labeling for de novo synthesized proteins after acid shock (Figure 1A). In the iron starvation experiment where complete medium replacement was necessary, conversion from 99At%[^{15}N] to 0.4At%[^{15}N] labeling was carried out to distinguish the old and the de novo synthesized proteins (Figure 1B). Cell samples were taken for analysis at one generation of growth after the stresses were applied.

In the acid shock experiment, *M. smegmatis* was grown in a 7H9 medium prepared from Sigma 7H9 base with 0.05% Tween 80 using glucose as a carbon source. Cultures were grown in 250-mL nephelo culture flasks under shaking at 37 °C. Growth was monitored by measuring turbidity in a Spec20 spectrometer. When the culture reached mid-log, it was doped with 0.5 g/L (final) 99At%[^{15}N]ammonium sulfate and partitioned into two flasks. Into one flask was added an appropriate amount of HCl to lower the pH to 5.0. The other flask was maintained at pH 7.0. Both cultures were grown until OD doubled, and cells were harvested for proteomic analysis.

In the iron starvation experiment, cells were grown in an [^{15}N] iron-rich 7H9 minimal medium containing (g/L) 99At%[^{15}N]$(NH_4)_2SO_4$, 0.5; glucose, 2; Tween 80, 0.5; citric acid, 0.094; biotin, 0.0005; pyridoxine, 0.001; NaCl, 0.1; Na_2HPO_4, 2.5; KH_2PO_4, 1; $MgSO_4 \cdot 6H_2O$, 0.1; $CuSO_4 \cdot 5H_2O$, 0.001; $ZnSO_4 \cdot 6H_2O$, 0.002; $CaCl_2 \cdot 2H_2O$, 0.0007; $FeCl_3$, 0.024; pH 7.0. A mid-log-phase culture was harvested by centrifugation at 4000 rpm in a refrigerated Eppendorf centrifuge. Two pellets were collected. The pellets were washed 3 times with ice-cold PBS. The two pellets were resuspended in a fresh [^{14}N] high-iron medium and a fresh [^{14}N] low-iron medium, respectively. The [^{14}N] high-iron medium was the same as the starting [^{15}N] iron-rich 7H9 minimal medium except that 0.4At%-[^{15}N]$(NH_4)_2SO_4$ was substituted for 99At%[^{15}N]$(NH_4)_2SO_4$. The [^{14}N] low-iron medium was prepared in the same way as the [^{14}N] high-iron medium except that the 0.024 g/L $FeCl_3$ component was omitted. The washed cell pellets were resuspended in these two fresh [^{14}N] media at OD 0.3−0.4. The resuspended cultures were grown at 37 °C until the OD doubled and cells were harvested for proteomic analysis. Since we did not validate the iron level in the medium without $FeCl_3$ by elemental analysis, we use the terms "low-iron" and "iron starvation" interchangeably within this context.

For LC−MS analysis, proteins were extracted from each cell pellet by bead beating using a protein extraction buffer that consisted of 100 mM ammonium bicarbonate (in the iron starvation experiment) or 0.05% SDS, 50 mM Tris, 5 mM EDTA, and 6 M urea (in the acid shock experiment). A protease inhibitor cocktail (Pierce, Rockford, IL) was added at 1× as recommended by the manufacturer into the mixtures of cell pellet and extraction buffer during protein extraction. The mixtures were vigorously agitated for total of 2 min at maximum speed in a Mini-BeadBeater (BioSpec, Bartlesville, OK) with 30 s of ice cooling at the 1-min intermittent time. The resulted mixtures were cleared by centrifugation at 13000*g* at 4 °C for 30 min and estimated for protein concentrations with BCA protein assay reagent (Pierce). About 60 μg of proteins was loaded for separation in each lane on a 10% Tris-HCl SDS-PAGE gel (Pierce). Gel bands were revealed by the Imperial Protein Stain (Pierce). Each lane of the gel was cut into five fractions. Gel pieces were minced to 1-mm^3 cubes, washed, and processed for in-gel digestion and peptide extraction as previously described.[15]

(10) Lessner, D. J.; Li, L.; Li, Q.; Rejtar, T.; Andreev, V. P.; Reichlen, M.; Hill, K.; Moran, J. J.; Karger, B. L.; Ferry, J. G. *Proc. Natl. Acad. Sci. U.S.A.* **2006**, *103*, 17921−17926.

(11) Li, L.; Li, Q.; Rohlin, L.; Kim, U.; Salmon, K.; Rejtar, T.; Gunsalus, R. P.; Karger, B. L.; Ferry, J. G. *J. Proteome Res.* **2007**, *6*, 759−771.

(12) de Godoy, L. M.; Olsen, J. V.; de Souza, G. A.; Li, G.; Mortensen, P.; Mann, M. *Genome Biol.* **2006**, *7*, R50.

(13) Voskuil, M. I.; Schnappinger, D.; Visconti, K. C.; Harrell, M. I.; Dolganov, G. M.; Sherman, D. R.; Schoolnik, G. K. *J. Exp. Med.* **2003**, *198*, 705−713.

(14) Amer, A. O.; Swanson, M. S. *Curr. Opin. Microbiol.* **2002**, *5*, 56−61.

(15) Li, Q.; Li, L.; Rejtar, T.; Lessner, D. J.; Karger, B. L.; Ferry, J. G. *J. Bacteriol.* **2006**, *188*, 702−710.

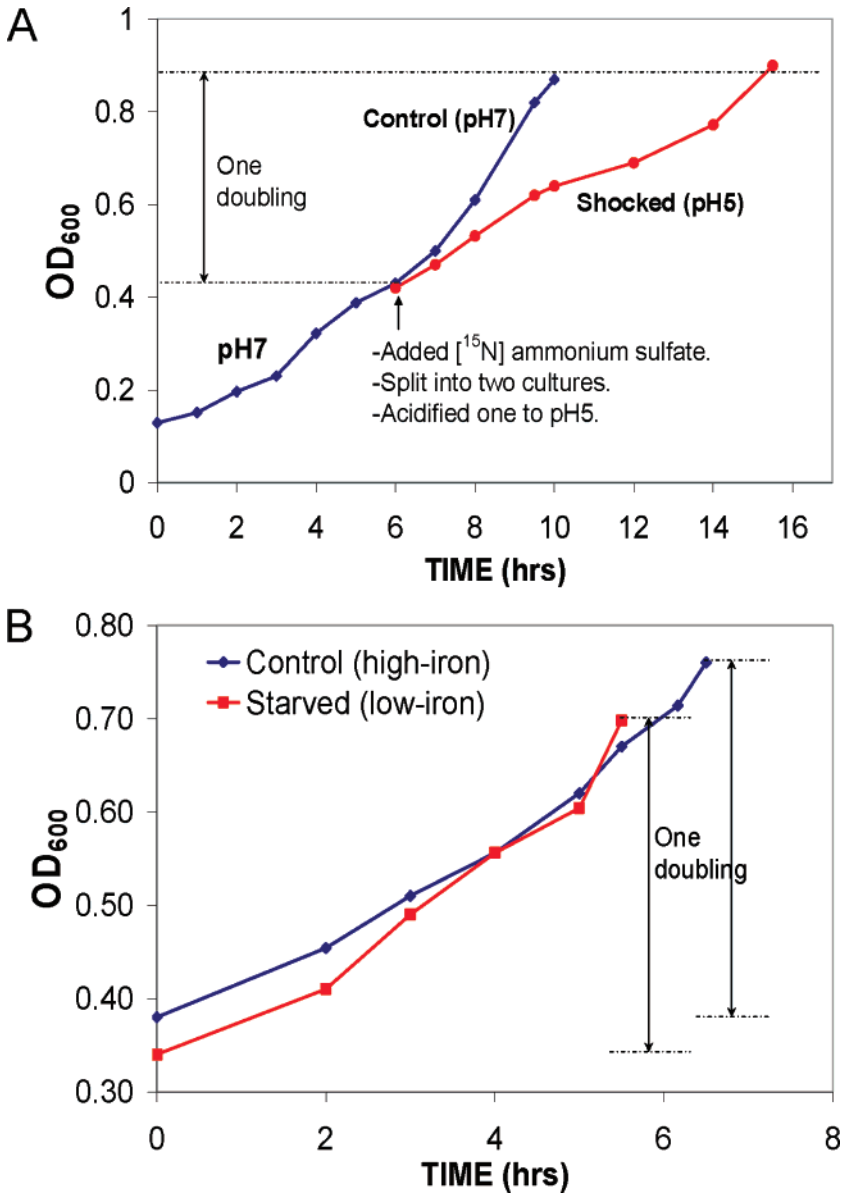

Figure 1. Representative growth curves for *M. smegmatis* in acid shock (A) and iron starvation (B) experiments.

Mass Spectrometry Analysis. Peptide extract samples were submitted to the Research Resource Center of University of Illinois at Chicago for protein identification on a nanoLC/LTQ-FT system. Peptide extracts were separated on a 75-μm-i.d. C18 reversed-phase column with a 5−35% acetonitrile (v/v) gradient in 0.1% TFA over 60 min and detected by the LTQ-FT. The LTQ-FT was operated in a data-dependent acquisition mode with up to 10 MSMS spectra acquired after each FTMS scan. Each SDS/PAGE fraction was analyzed once. The acquired RAW data files were searched against the *M. smegmatis* strain mc^2 155 NCBI database in two separate BioWorks searches, one corresponding to [^{14}N] and the other [^{15}N] labeling. The precursor ion tolerance was set to ±1.5 Da, and digestion enzyme was designated as trypsin with two missed cleavages allowed. Peptide and protein probabilities were calculated in BioWorks. Only peptides with p <0.01 were used for subsequent quantitation analysis.

Data Analysis. The protein quantitation procedure was based upon the previously described QN algorithm.[9] The program was kindly provided by Dr. Barry L. Karger's laboratory at Northeastern University under open license and was modified in Matlab v7.2 environment to accommodate calculation of isotopologue abundances at different atomic percent [^{15}N] labeling other than near unity and to use peptide and protein probabilities calculated by BioWorks (Finnigan, San Jose, CA). S/D was calculated for every identified peptide charge state[9] with p <0.01. Multiple peptide charge states for the same protein were filtered for outlier S/D by Dixon's Q-test (95% confidence level) before being used to calculate the S/D for the protein. S/D was calculated only for proteins with at least two qualified peptide-charge-state identifications. The S/D quantitation procedure was essentially the same as that used for differential expression analysis,[9,15] but with the added functionality to compute S/D for different isotopomer profiles with different [^{15}N] abundance in a medium, as shown in Figure 2.

In Figure 2, we use a representative tryptic peptide ANLLGLSAPEMTTLVGGLR to illustrate the calculation of S/D for the four culture samples harvested from the two different experiments. This peptide is from a catalase/peroxidase (MSMEG6346; KatG)

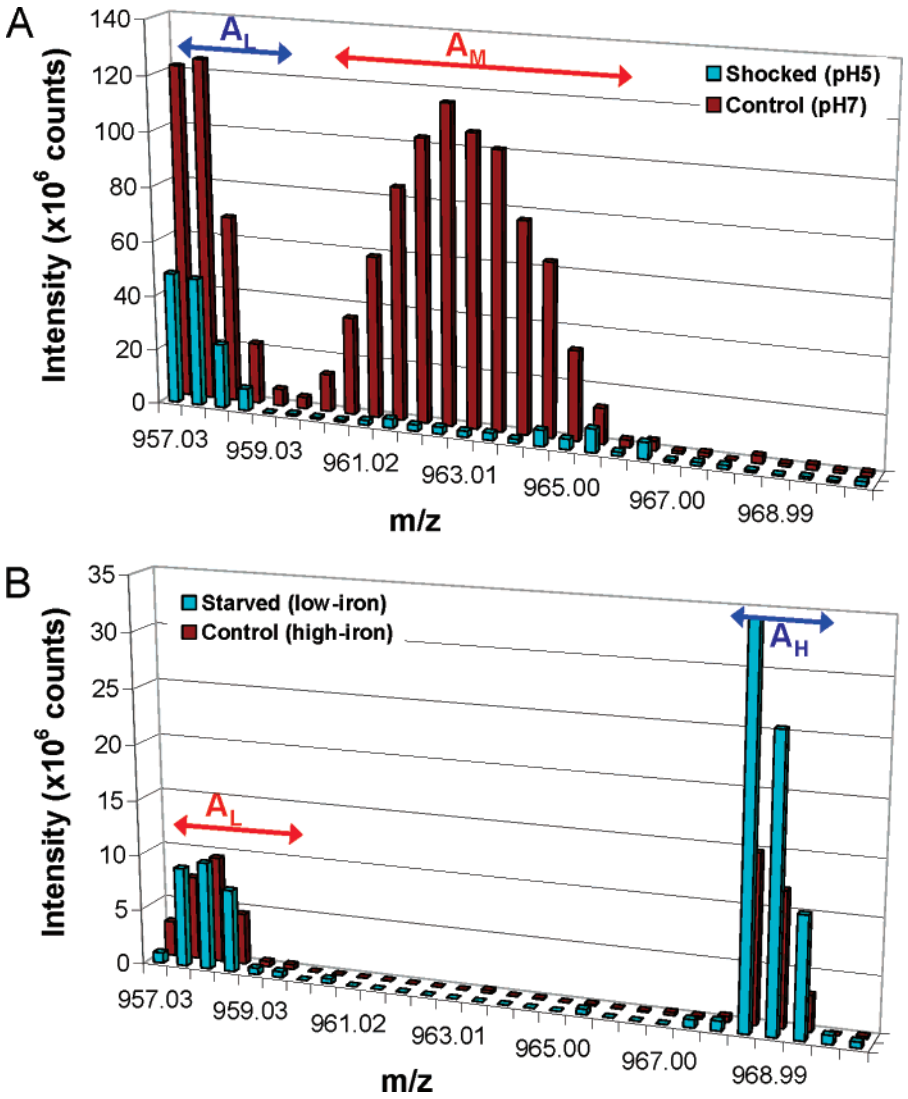

Figure 2. Calculation of isotopologue intensities for a representative tryptic peptide ANLLGLSAPEMTTLVGGLR (MH_2^{2+}, 23 N atoms) of protein KatG (MSMEG6346) in shocked (pH5) and control (pH7) cultures (panel A) and in starved (low-iron) and control (high-iron) cultures (panel B). A_L, A_H, and A_M represent the isotopologue intensities with light label (99.6At%[^{14}N]), heavy label (99At%[^{15}N]), and medium label (50At%[^{15}N]), respectively. Red arrows and text labels indicate de novo synthesized proteins. Blue arrows and text labels indicate old proteins. See text for more details.

and contains 23 N atoms. Shown in Figure 2 are the [^{14}N]/[^{15}N]-labeled isotopologue pairs of the charge state +2 of this peptide from the four culture samples, namely, the pH 5 shocked and the pH 7 control (panel A), and the low-iron starved and the high-iron control (panel B). The *x*-axis (m/z) represents the m/z of the isotopomer peaks with [^{15}N] dilution. The first isotopomer corresponds to the [^{14}N] label monoisotopic peak. The *z*-axis (intensity) represents individual isotopomer peak intensities. An isotopomer peak intensity was calculated by integrating the full isotopomer peak area from an averaged MS spectrum summing 120 FTMS scans covering the chromatographic elution time window of the peptide. The *y*-axis (not labeled) represents different culture conditions that are labeled in the legends. The arrows indicate the isotopomer ranges for integrating the intensities (denoted by letter A) of different isotopologues (denoted with different subscript letters). A_L, A_H, and A_M represent the isotopologue intensities with light label (99.6At%[^{14}N]), heavy label (99At%[^{15}N]), and medium label (50At%[^{15}N]), respectively. The red arrows and text labels indicate de novo synthesized proteins, and the blue arrows and text labels indicate old proteins. For the acid shock experiment, S/D = A_M/A_L. For the iron starvation experiment, S/D = A_L/A_H.

For automated calculation of S/D for all the proteins, we first examined the isotopomer profiles for the identified peptides. There were total 1753 and 1974 detected peptide charge states (p <0.01) in the acid shock and iron starvation experiments, respectively. The histograms of the number of N atoms in peptides were constructed for these peptide charge states in the two experiments, respectively (Figure 3). Based on the histograms, we constructed an average isotopomer profile for the peptide charge states with the same number of N atoms. This was done by first normalizing an isotopomer profile with the sum of the isotopomer intensities in that profile. Then the normalized isotopomer profiles with the same number of N atoms were plotted in an Excel stacked column graph to represent the average isotopomer profile. Figure 4 shows four representative average isotopomer profiles for the number of N atoms of 11, 16, 20, and 25. From these average isotopomer profiles, the isotopomer boundaries for isotopologue

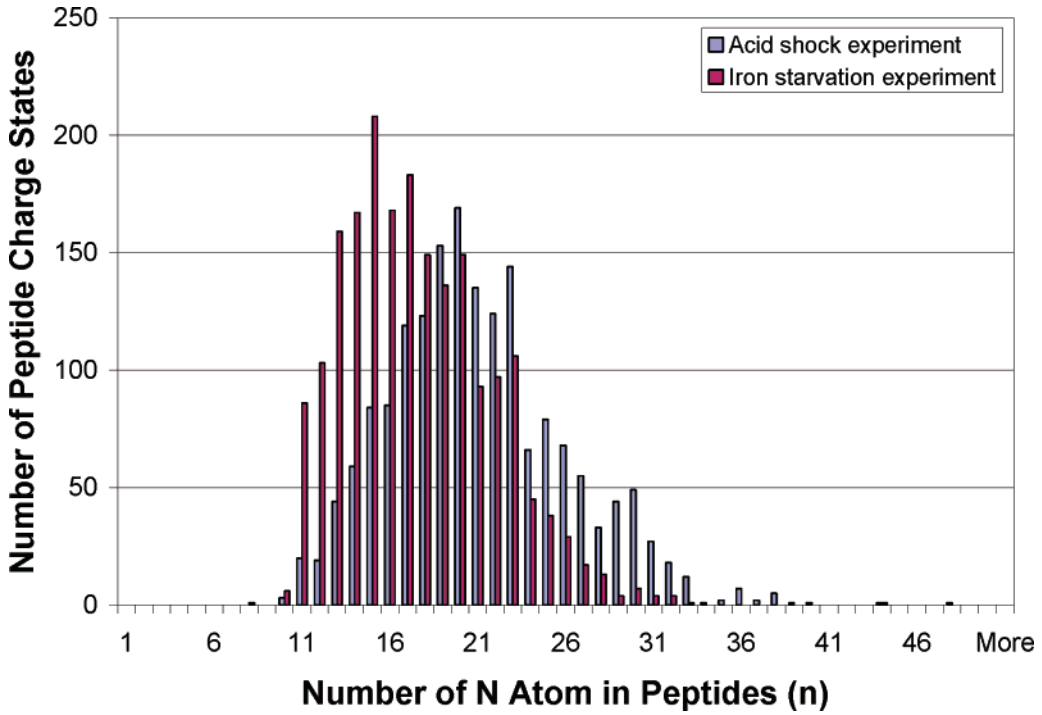

Figure 3. Histograms of number of N atoms in all the identified peptide charge states (p <0.01) in the acid shock and the iron starvation experiments.

Table 1. Selection of Isotopomer Number (M) Ranges for Calculating A_L, A_H, and A_M at Different Number of N Atoms (n) for All the Identified Peptide Charge States in the Two Experiments

	M ranges for isotopologue intensity calculation			
	acid shock experiment		iron starvation experiment	
n	A_L	A_M	A_L	A_H
10−12	1−2	$4-n-3$	1−4	$n+1-n+3$
13−18	1−3	$5-n-3$	1−5	$n+1-n+3$
19−21	1−4	$6-n-3$	1−6	$n+1-n+3$
22−27	1−5	$7-n-3$	1−7	$n+1-n+3$
28−48	1−6	$8-n-3$	1−8	$n+1-n+3$

intensity calculation were defined empirically and shown in Figure 4. Table 1 summarizes the complete scheme of selecting the isotopomer ranges for calculating A_L, A_H, and A_M at all possible numbers of N atoms for the identified peptide charge states. From Figure 4, it can be seen that the A_L isotopologue profiles in the ion starvation experiment were shifted toward a slightly higher [^{15}N] enrichment compared to the natural [^{14}N] abundance. This could be due to carryover of extracellular [^{15}N]$(NH_4)_2SO_4$ from the media during medium replacement or recycling of intracellular [^{15}N] amino acids or ammonium precursors after medium replacement. This will be investigated in future work. Nevertheless, the shift did not affect the isotopologue intensity calculation after implementing the isotopomer range selection scheme shown in Table 1.

Upon calculating the S/D for all the detected peptide charge states, the S/D was calculated for the corresponding proteins in a manner similar to that in the differential abundance measurement.[9] The coefficient of variance (CV) distributions for protein S/D measurement in all of the four cultures were as expected with average CV from 11 to 16% and median CV from 8 to 11% (Figure 5). This was consistent with the previous study.[9] The procedure thus demonstrates the confidence necessary for automated global S/D measurements.

RESULTS AND DISCUSION

We demonstrated protein turnover measurement at a global level for *M. smegmatis* under acid shock and iron starvation conditions, taking advantage of the high resolution and mass accuracy of the LTQ-FT mass spectrometer.

There were 194, 118, 142, and 155 proteins quantified in the pH 7, pH 5, high-iron, and low-iron culture cells, respectively, constituting a total 247 proteins detected from the four cultures. Of these 247 proteins, 114 were found in both the pH 5 and the pH 7 culture cells, 121 in both the low-iron and the high-iron culture cells, and 84 in all the four culture cells. As listed in Table S1 (Supporting Information, SI), there were 151 proteins with S/D determined in at least one pair of culture cells in the same experiment. A pair of culture cells means the stressed and the control cells in either the acid shock or the iron starvation experiment. Protein turnover was represented by the S/D.[5] Of the 151 proteins, 84 proteins have S/D determined in both pairs of culture cells and 67 proteins have S/D determined in at least one but not both pairs of culture cells. The distribution of S/D measurement CV% for the four different culture samples is presented in Figure 5, illustrating that both the isotope doping and the complete medium replacement method for metabolic labeling worked similarly well in regard to measurement precision. The average and the median CV% for both of the cultures in the iron starvation experiment were slightly better than those in the acid shock experiment (data not shown), probably because of

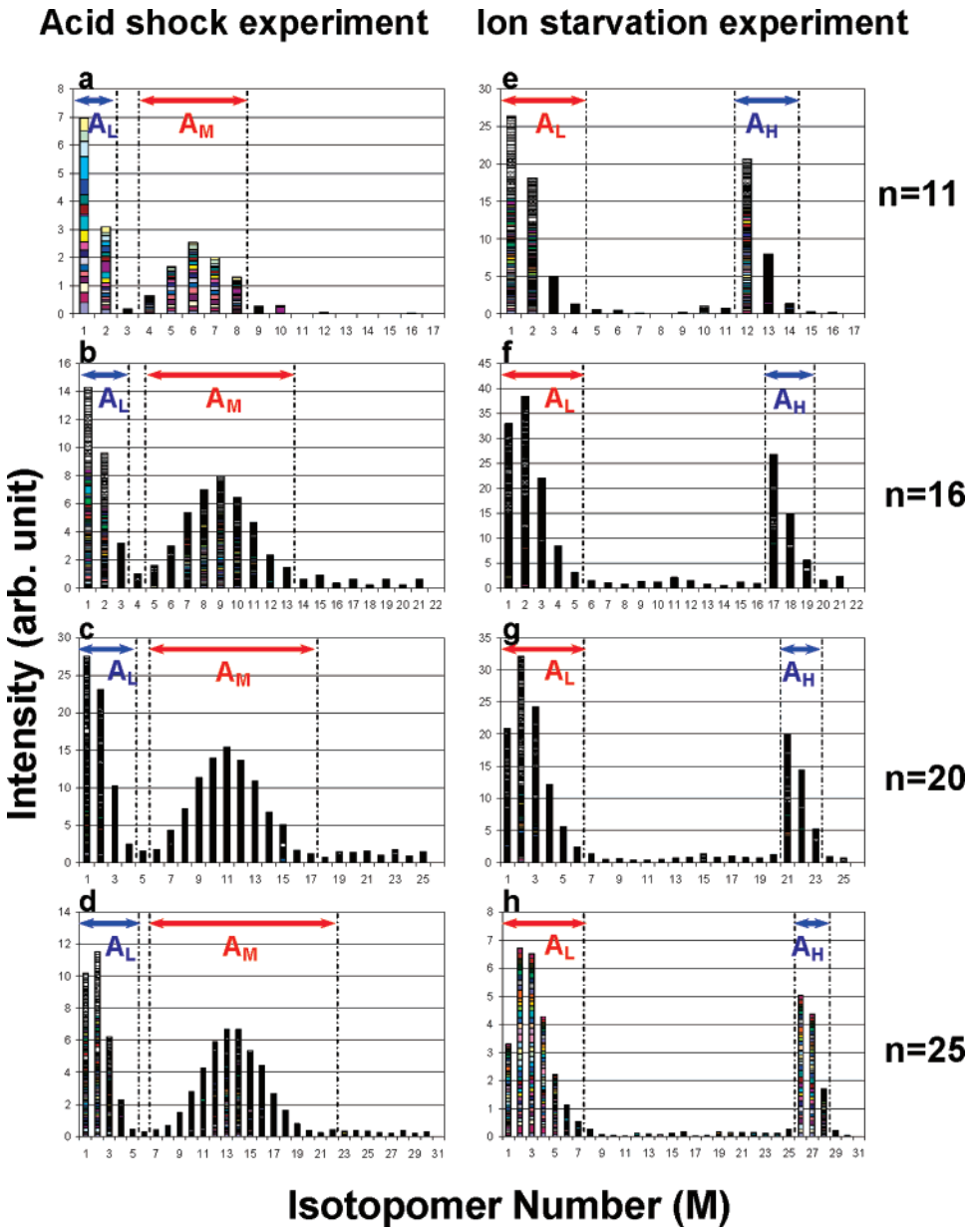

Figure 4. Average isotopomer profiles and selected isotopomer ranges for calculating A_L, A_H, and A_M when the number of N atoms (n) was equal to 11 (a and e), 16 (b and f), 20 (c and g), and 25 (d and h) in the two experiments. From panel a to h, each panel was the stacked column graph of the normalized isotopomer profiles of the detected peptide charge states having the same number of N atoms. A_L, A_H, and A_M are as defined in Figure 2, with blue text representing old proteins and red for de novo synthesized proteins. The blue and red arrows indicate the isotopomer ranges selected for calculating the isotopologue intensities for the old and the de novo synthesized proteins respectively. For the acid shock experiment, S/D = A_M/A_L. For the iron starvation experiment, S/D = A_L/A_H.

the more disbursed isotopomer profiles in the acid shock experiment where de novo synthesized proteins were labeled at 50At%-[^{15}N]. A more disbursed isotopologue profile lowers signal-to-noise ratio compared to a tighter one when the isotopic labeling is near unity atomic percent.

First, we compared the global protein turnover profiles of *M. smegmatis* cells under the acid shock and the iron starvation conditions (Figure 6). One of the most noticeable differences between these two stress conditions is the correlation of S/D between the stressed and the control cells. The correlation was very large in the iron starvation experiment but small in the acid shock experiment (Table 2). This suggests that the S/D for many proteins in the pH 5 cells underwent significant readjustment in different directions, while the S/D for most proteins remained similar or shifted in the same direction when the cells were shifted from high- to low-iron media. This illustrates that S/D measurement provides interesting insight into the dynamic nature of cell stress response. Comparison of other different pairings among the four culture samples revealed trivial correlation (Table 2). It was surprising to note that the two control samples showed trivial correlation even though both were at pH 7.0. As described in Materials and Methods, these two control cultures differed mainly in that one contained glutamic acid and the other did not. These observations again indicate that the presence and the absence of glutamic acid in the culture medium have greater influence on the S/D than a change in either pH or iron concentration alone. This notion is further supported by our protein relative abundance ratio analysis of ~570 proteins among the cells grown in the Sigma

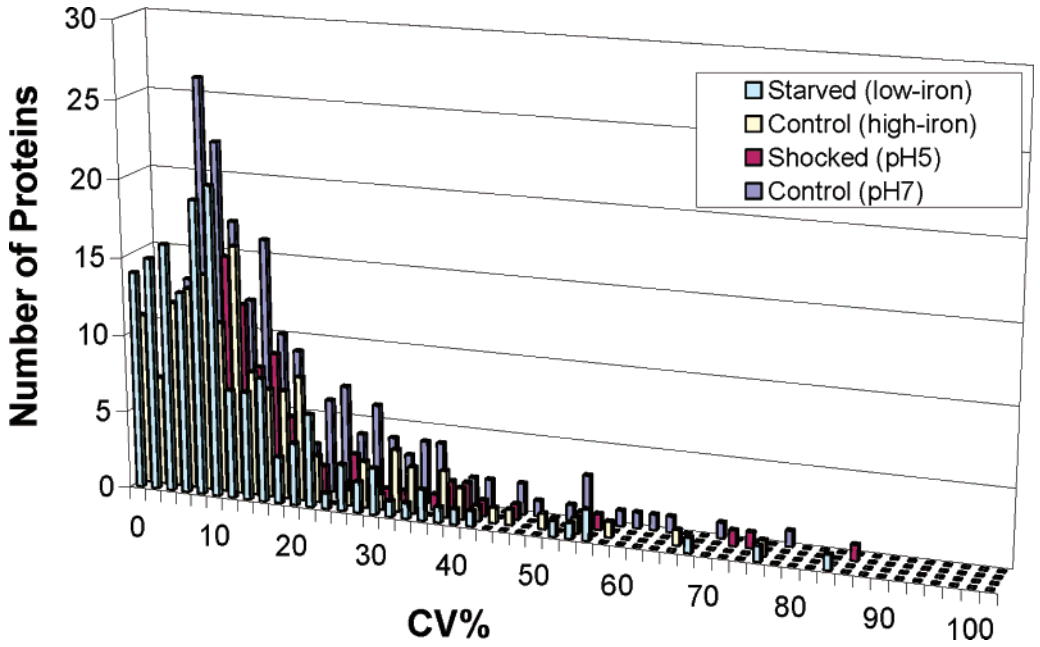

Figure 5. CV% histograms of S/D measurement for the four culture samples.

7H9 broth at pH 5.0 and pH 7.0 and the cells grown in a 7H9 minimal medium without glutamic acid at pH 5.0. In that study, more proteins were found to be regulated between the Sigma 7H9 broth grown and the minimal 7H9 medium grown cells than between the pH 5.0 and the pH 7.0 Sigma 7H9 culture cells (Roxas and Li, unpublished data).

As can be seen from Figure 6, the results of protein turnover measurement indicate that the approach used here is capable of measuring S/D over a dynamic range of 3 orders of magnitude. It was noted that the lowest S/D was 0.20 ± 0.05 for bacterioferritin (MSMEG3564; Bfr) in the low-iron starved culture and 0.18 ± 0.05 for ATP synthase b chain (MSMEG4926; AtpF) in the acid shocked culture. The highest S/D was 521 ± 97 for glycerol kinase (MSMEG6190; GlpK) in the high-iron control culture (Table S1, SI). The narrower S/D dynamic range of 2 orders of magnitude observed in the acid shock experiment was probably because the highest turnover proteins were not identified by the mass spectrometry due to the 50At%[^{15}N] medium labeling. But it cannot be excluded that the narrower dynamic range was also inherent to biological properties of the cells. This will need further experiments to clarify. Interestingly, a glycerol kinase (MSMEG6720; GlpK) had S/D of 240 and 270 in the iron starvation experiment but only 1.2 and 2.8 in the acid shock experiment (Table S1, SI), suggesting that protein turnover is highly dependent upon culture media or experimental conditions for some proteins.

As a simplified scenario, we propose that changes in protein S/D have the following implications for a culture growing logarithmically by one doubling. Assuming zero protein degradation, a culture logarithmically growing by one generation would yield S/D of unity. Deviation from unity in S/D occurs when protein degradation comes into play or de novo protein synthesis is under new regulation. Upregulation in protein de novo synthesis will apparently increase S/D to more than 1. Protein degradation will further increase S/D when de novo protein synthesis is upregulated, reflecting active protein turnover. Thus, a significant increase in S/D could be due to protein synthesis upregulation alone or in combination with protein degradation. When there is significant downregulation in de novo protein synthesis, S/D will decrease to less than 1. As in a typical quantitative proteomic analysis, hereafter, we use 2-fold difference as the threshold for distinguishing a protein that underwent active turnover versus those that did not. Likewise, we also use 2-fold as an arbitrary cutoff when comparing the S/D under one versus another condition.

Figure 6A reveals that none of the proteins in the pH 7 control cells and only two proteins (MSMEG4926 and MSMEG6139) in the pH 5 acid stressed cells had S/D below 0.5. Similarly, in Figure 6B, none of the proteins in the high-iron control cells and only two proteins (MSMEG3564 and MSMEG6346) in the low-iron starved cells had S/D below 0.5. This suggests that most of the proteins experienced active degradation or upregulation of de novo synthesis in the pH 7 control and the low-iron stressed cells that led to an increase in S/D to above unity.

There were 12 of 131 (9%), 64 of 116 (55%), 108 of 129 (84%), and 29 of 126 (23%) proteins with S/D > 2 in the pH 7 control, pH 5 stressed, high-iron control, and low-iron starved culture cells respectively (Table S1, SI). While the pH 7 control cells had only 9% of the proteins with S/D > 2, the high-iron control cells had 84% of the proteins with S/D > 2. While both control cultures in the acid shock and the iron starvation experiments were at pH 7.0, one difference was that the media for acid shock experiment were made from the Sigma 7H9 broth, and the media for the iron starvation experiment were laboratory-made based on the Sigma 7H9 broth formulation with glutamic acid omitted (see Materials and Methods). The doubling time for the pH 7 control culture was 4.0 h while that for the high-iron control culture was 6.5 h (Figure 1). The pH 5 stressed cells had 55% of the proteins with S/D > 2, and the low-iron starved cells had 23%. Their doubling times were 9.5 and 5.5 h, respectively. Slower culture growth is typically associated with higher protein degradation rates.[1] This may be one of the reasons why the pH 5 stressed cells and the

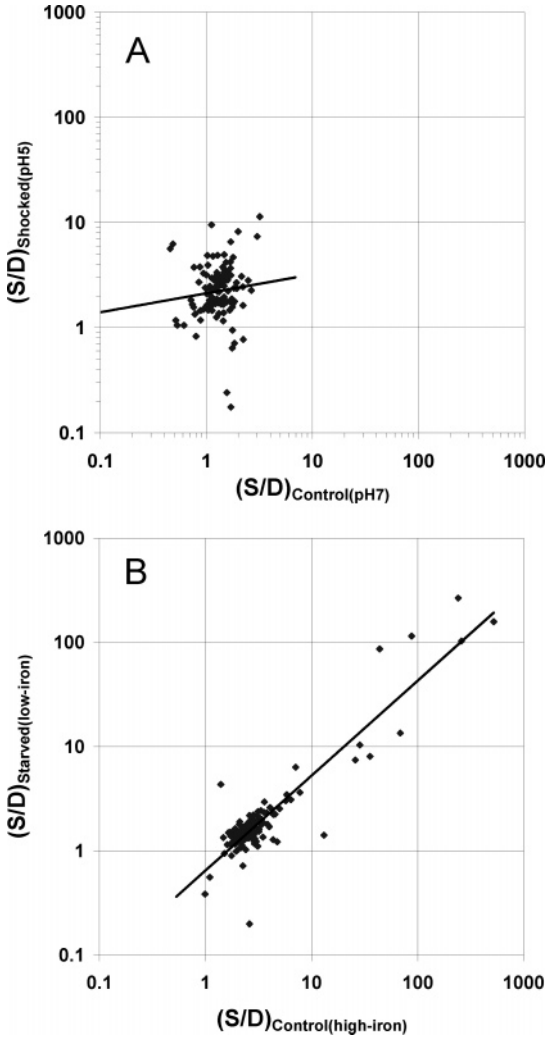

Figure 6. S/D scatter plots. Panel A: 114 proteins quantified in both acid shocked (pH5) and control (pH7) *M. smegmatis* cells. Panel B: 121 proteins quantified in both starved (low-iron) and control (high-iron) *M. smegmatis* cells. The regression lines indicate the correlation between the stressed and the control cells. The Pearson's correlation coefficient was 0.27 in panel A and 0.81 in panel B.

Table 2. Pearson's Correlation Coefficients of S/D among the Four Culture Cells, Calculated for the 151 Proteins Listed in Table S1 (SI)

	shocked (pH 5)	control (high-iron)	starved (low-iron)
control (pH 7)	0.27	0.05	−0.02
shocked (pH 5)	1	0.03	0.02
control (high−iron)	−	1	0.81

high-iron control cells had higher percentage of high S/D proteins. But, we cannot exclude other possibilities. For example, the pH 5 stressed cells were under acid shock. They needed to upregulate the synthesis of new proteins to prepare the cells to cope with the acid stress[16] and probably also accelerated degradation of some unneeded proteins under the new acidic condition. Both processes would increase the S/D. The lower percentage of high S/D proteins in the low-iron starved cells compared to that of the high-iron control cells could be due to slowdown of de novo protein synthesis, stabilization of proteins, or secretion/excretion of some de novo synthesized proteins or siderophores to the extracellular medium during iron starvation.[17] Although the data we have obtained in this work were not intended to resolve all these questions, it reveals the complexity of dynamic cell response to stressful conditions. Combination of protein relative abundance and turnover kinetic measurements will be able to provide more in-depth insight into the dynamic nature of a proteome.

Second, we compare the changes of S/D between the stressed and the control cells in the acid shock and the iron starvation experiments. Of the 84 proteins detected in all four cultures, 31 had statistically significant S/D changes in both experiments and had S/D changed by more than 2-fold in at least one of the two experiments (Table 3). Figure 7 shows the scatter plot of $(S/D)_{LoFe}/(S/D)_{HiFe}$ versus $(S/D)_{pH5}/(S/D)_{pH7}$ for the 31 proteins listed in Table 3. It is striking to note that $(S/D)_{LoFe}/(S/D)_{HiFe}$ were below one for all these 31 proteins. On the contrary, all the 31 but 2 proteins had $(S/D)_{pH5}/(S/D)_{pH7}$ greater than one. For these 31 proteins, the Pearson's correlation coefficient between $(S/D)_{pH5}$ and $(S/D)_{pH7}$ was 0.67 and that between $(S/D)_{LoFe}$ and $(S/D)_{HiFe}$ was 0.87, again supporting the earlier view that the proteins under acid shock underwent more significant readjustment in protein turnover. Interestingly, other pairings among the four culture samples all revealed moderate correlations (Table 4). This is apparently different from what was observed when the 151 proteins were taken for correlation analysis (Table 2). Many of these 31 proteins may have coordinated response to stresses due to their roles in common processes affected by the stresses. Indeed, 12 proteins have roles in transcription and translation. At least 10 proteins are metabolic enzymes. Three proteins are related to oxidative stress response and one involves energy conservation.

Of the 31 proteins in Table 3, catalase/peroxidase (MSMEG6346; KatG) and ATP synthase F1 β subunit (MSMEG4921; AtpD) were the only two proteins having both $(S/D)_{LoFe}/(S/D)_{HiFe}$ and $(S/D)_{pH5}/(S/D)_{pH7}$ less than 0.5 (Figure 7). This suggests a decrease in protein turnover and downregulation of de novo synthesis for these two proteins under both stress conditions. Although *M. smegamatis* strain mc^2 155 has three KatG paralogues in the genome and had two KatG paralogues detected (Table S1, SI), MSMEG6346 has the highest identity with the only copy of KatG (Rv1908c) in *M. tuberculosis* H37Rv (www.tigr.org). Slowdown of protein turnover for AtpD at both stress conditions suggests that ATP synthesis may be decreased under the stress conditions.

KatG has an indispensable role in *M. tuberculosis* pathogenesis by catabolizing the ROS during phagocyte oxidative burst, which is a major host defense against pathogen infection, while it is dispensable in the absence of the this host antimicrobial mechanism.[18] KatG is one of the several key enzymes comprising the mycobacterial ROS detoxification system.[19,20] It was proposed to function as a peroxynitritase neutralizing the highly reactive

(16) O'Brien, L. M.; Gordon, S. V.; Roberts, I. S.; Andrew, P. W. *FEMS Microbiol. Lett.* **1996**, *139*, 11−17.

(17) Rodriguez, G. M. *Trends Microbiol.* **2006**, *14*, 320−327.

(18) Ng, V. H.; Cox, J. S.; Sousa, A. O.; MacMicking, J. D.; McKinney, J. D. *Mol. Microbiol.* **2004**, *52*, 1291−1302.

(19) Milano, A.; Forti, F.; Sala, C.; Riccardi, G.; Ghisotti, D. *J. Bacteriol.* **2001**, *183*, 6801−6806.

(20) Zahrt, T. C.; Song, J.; Siple, J.; Deretic, V. *Mol. Microbiol.* **2001**, *39*, 1174−1185.

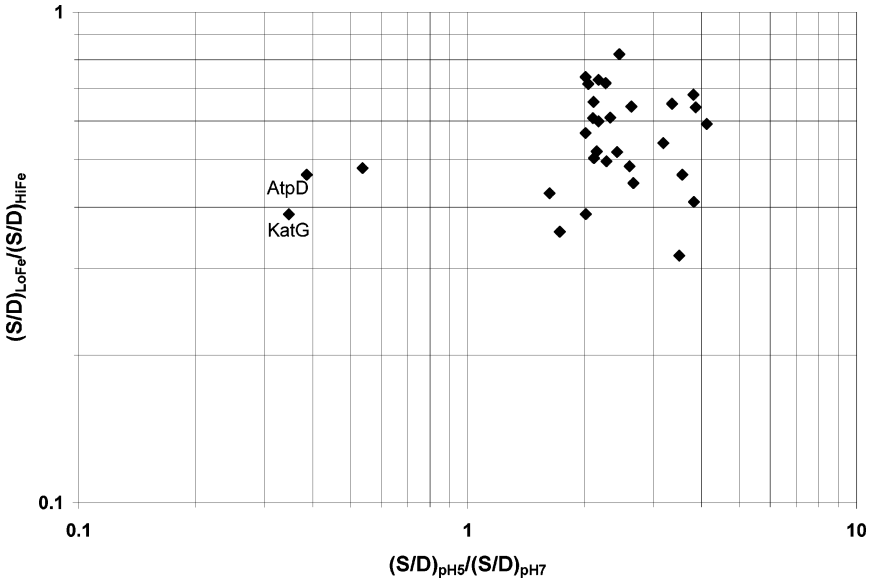

Figure 7. Scatter plot of $(S/D)_{LoFe}/(S/D)_{HiFe}$ versus $(S/D)_{pH5}/(S/D)_{pH7}$ for the 31 proteins listed in Table 3. HiFe, high-iron. LoFe, low-iron. Only two proteins, catalase/peroxidase (MSMEG6346; KatG) and ATP synthase F1 β subunit (MSMEG4921; AtpD) had both $(S/D)_{LoFe}/(S/D)_{HiFe}$ and $(S/D)_{pH5}/(S/D)_{pH7}$ less than 0.5, as labeled in the graph.

oxidant peroxynitrous acid (ONOOH) resulting from the reaction of the superoxide anion ($O_2^{\bullet}$) and nitric oxide (NO).[21]

Isoniazid, a frontline antituberculosis antibiotic, is a prodrug that requires activation by KatG in conjunction with hydrogen peroxide to be bacterialcidal.[22,23] Activation of isoniazid, however, also generates oxidative species[24] that in turn induces mycobacterial dormancy.[13] This coincides with the fact that isoniazid is highly efficient in killing 99% of actively growing mycobacteria but is ineffective against the remaining dormant subpopulation.[25,26] The action mechanism of isoniazid remains a perplexing topic for ongoing studies[27] even though half a century has passed since the discovery of this drug.[28]

Isoniazid induces oxidative stress and dormancy in *M. tuberculosis*.[13,24] It was found that KatG was downregulated in *M. tuberculosis* by 30-fold upon treatment with isoniazid.[29] Dormancy is an important survival tactic for microbes in pathogenesis and in other natural environments where stressful conditions are more the rule than the exception. Using the proteomic approach in this work, we found that protein turnover was lowered for KatG when *M. smegmatis* encountered stressful conditions. This may explain why isoniazid is ineffective against the cells entering dormancy under stress.[25,26] The approach demonstrated here potentially can be applied to evaluate drug targets at various stress conditions mimicking the microenvironments encountered by a pathogen inside a host, complementing common procedures where a drug is typically tested against an actively growing laboratory culture.

In addition to KatG, two other related proteins of the mycobacterial ROS detoxification system[19,20] were also detected with reduced S/D under the low-iron condition, namely, superoxide dismutase (Mn; MSMEG6390) and thiol peroxidase (Tpx; MSMEG3484) (Table 3). The turnover of Tpx was also reduced in the acid shocked cells.

Superoxide dismutase has been implicated in protecting *M. tuberculosis* against ROS, which is an important strategy employed by host cells for overcoming infection. MSMEG6390 has 81.2% identity and 89.9% similarity with the superoxide dismutase (Fe) (SodA; Rv3846) in *M. tuberculosis*. SodA uses iron as a cofactor and imparts significant protection against ROS. In addition, it also induces an immune response in the host due to the presence of B-cell epitopes. It was demonstrated that the bacillary load of infected animal organs was reduced by 2−3 log when the *sodA* gene was rendered nonfunctional by antisense strategy.[30] It was postulated that an antigen like SodA may have dual function; i.e., it may have a role in pathogenesis as well as may provide protection against the infection, depending upon its use.[31] Our finding of lower S/D value for Mn at low-iron condition is consistent with the view that limitation of iron source has an effect on *M. tuberculosis* pathogenesis and host immune response.

The *M. smegmatis* Tpx (MSMEG3484) has 84.8% identity and 91.5% similarity to the *M. tuberculosis* Tpx (Rv1932). Tpx is structurally homologous to other peroxiredoxins, including the mycobacterial AhpC that constitutively expresses in isoniazid

(21) Wengenack, N. L.; Jensen, M. P.; Rusnak, F.; Stern, M. K. *Biochem. Biophys. Res. Commun.* **1999**, *256*, 485−487.
(22) Timmins, G. S.; Master, S.; Rusnak, F.; Deretic, V. *J. Bacteriol.* **2004**, *186*, 5427−5431.
(23) Hochleitner, E. O.; Kastner, B.; Frohlich, T.; Schmidt, A.; Luhrmann, R.; Arnold, G.; Lottspeich, F. *J. Biol. Chem.* **2005**, *280*, 2536−2542.
(24) Timmins, G. S.; Master, S.; Rusnak, F.; Deretic, V. *Antimicrob. Agents Chemother.* **2004**, *48*, 3006−3009.
(25) Wayne, L. G.; Sramek, H. A. *Antimicrob. Agents Chemother.* **1994**, *38*, 2054−2058.
(26) Papadopoulou, M. V.; Bloomer, W. D.; McNeil, M. R. *Int. J. Antimicrob. Agents* **2007**, *29*, 724−727.
(27) Dias, M. V.; Vasconcelos, I. B.; Prado, A. M.; Fadel, V.; Basso, L. A.; de Azevedo, W. F., Jr.; Santos, D. S. *J. Struct. Biol.* **2007**, May 3; [Epub ahead of print].
(28) Bernstein, J.; Lott, W. A.; Steinberg, B. A.; Yale, H. L. *Am. Rev. Tuberculosis.* **1952**, *65*, 357−364.
(29) Hughes, M. A.; Silva, J. C.; Geromanos, S. J.; Townsend, C. A. *J. Proteome Res.* **2006**, *5*, 54−63.
(30) Edwards, K. M.; Cynamon, M. H.; Voladri, R. K.; Hager, C. C.; DeStefano, M. S.; Tham, K. T.; Lakey, D. L.; Bochan, M. R.; Kernodle, D. S. *Am. J. Respir. Crit. Care Med.* **2001**, *164*, 2213−2219.
(31) Register, K. B. *Vaccine* **2004**, *23*, 48−57.

Table 3. List of 31 Proteins That Had Statistically Significant S/D Changes (p <0.05) in Both Experiments and Had More than 2-Fold Change in S/D in at Least One Experiment[a]

		acid shock				iron starvation			
locus	protein name	$(S/D)_{pH7}$	$(S/D)_{pH5}$	R_{pH}	p	$(S/D)_{HiFe}$	$(S/D)_{LoFe}$	R_{Iron}	p
0697	luciferase−like monooxygenase superfamily	1.3 ± 0.3	4.9 ± 0.1	3.8	<0.01	3.0 ± 0.2	1.2 ± 0.2	0.41	<0.01
0772	F420−dependent glucose−6−phosphate dehydrogenase (mer−2)	1.5 ± 0.7	4.9 ± 0.3	3.4	<0.01	2.6 ± 0.1	1.7 ± 0.0	0.65	<0.01
0906	methoxy mycolic acid synthase 1 (umaA1)	1.8 ± 0.1	4.7 ± 0.7	2.6	<0.01	6.4 ± 0.2	3.1 ± 0.3	0.48	<0.01
1340	ribosomal protein L1 (rplA)	1.2 ± 0.1	2.4 ± 0.2	2.0	<0.01	2.6 ± 0.4	1.9 ± 0.1	0.74	<0.01
1360	DNA polymerase (rpoB) (rpoB)	2.0 ± 0.2	8.2 ± 0.3	4.1	<0.01	5.8 ± 0.4	3.4 ± 0.1	0.59	<0.01
1361	DNA−directed RNA polymerase, β' subunit (rpoC)	1.7 ± 0.1	7 ± 1	4	<0.01	4.1 ± 0.3	2.6 ± 0.1	0.64	<0.01
1434	ribosomal protein L3 (rplC)	0.7 ± 0.1	1.7 ± 0.2	2.3	<0.01	1.9 ± 0.0	1.3 ± 0.1	0.72	<0.01
1437	ribosomal protein L2 (rplB)	1.0 ± 0.2	1.6 ± 0.2	1.6	<0.01	4.0 ± 1.1	1.7 ± 0.3	0.4	<0.01
1443	rpsQ (rpsQ)	0.8 ± 0.1	1.4 ± 0.2	1.7	<0.01	3.1 ± 0.1	1.1 ± 0.1	0.36	<0.01
1523	DNA−directed RNA polymerase, α subunit	1.2 ± 0.1	2.4 ± 0.3	2.0	<0.01	2.6 ± 0.4	1.4 ± 0.1	0.57	<0.01
2373	ketol−acid reductoisomerase (ilvC)	1.1 ± 0.1	3.0 ± 0.0	2.6	<0.01	2.8 ± 0.3	1.8 ± 0.2	0.64	<0.01
2377	D−3−phosphoglycerate dehydrogenase (serA)	1.3 ± 0.2	3.3 ± 0.5	2.7	<0.01	2.9 ± 0.3	1.3 ± 0.0	0.45	<0.01
2522	ribosomal protein S2 (rpsB)	0.8 ± 0.1	2.7 ± 0.7	3.2	<0.01	2.7 ± 0.0	1.5 ± 0.1	0.54	<0.01
2653	ribosomal protein S15 (rpsO)	0.5 ± 0.1	1.2 ± 0.3	2.3	<0.01	2.1 ± 0.3	1.1 ± 0.1	0.50	<0.01
3066	S−adenosylmethionine synthetase (metK)	1.3 ± 0.1	2.8 ± 0.2	2.1	<0.01	2.5 ± 0.3	1.3 ± 0.3	0.52	<0.01
3151	acn (acn)	0.9 ± 0.3	3.3 ± 0.6	3.5	<0.01	2.2 ± 0.1	0.7 ± 0.1	0.32	<0.01
3237	pyruvate kinase (pyk)	1.6 ± 0.3	3.3 ± 0.2	2.1	<0.01	3.2 ± 1.0	1.6 ± 0.1	0.50	0.01
3484	thiol peroxidase (tpx)	1.8 ± 0.0	0.9 ± 0.3	0.54	0.03	3.2 ± 0.4	1.5 ± 0.1	0.48	<0.01
3838	rpsA (rpsA)	1.3 ± 0.1	2.7 ± 0.1	2.1	<0.01	3.6 ± 0.4	2.3 ± 0.2	0.66	<0.01
4293	glutamine synthetase, type I (glnA)	1.1 ± 0.1	2.3 ± 0.2	2.0	<0.01	1.6 ± 0.1	1.1 ± 0.1	0.71	<0.01
4616	ribosomal protein L27 (rpmA)	1.3 ± 0.2	3.1 ± 0.0	2.3	<0.01	2.3 ± 0.4	1.4 ± 0.4	0.61	<0.01
4747	fatty−acid synthase (fas)	3.2 ± 0.1	11 ± 1	3.6	<0.01	7.8 ± 0.4	3.6 ± 0.1	0.47	<0.01
4921	ATP synthase F1, beta subunit (atpD)	1.8 ± 0.1	0.7 ± 0.1	0.39	<0.01	3.8 ± 0.8	1.8 ± 0.1	0.47	<0.01
5037	2−oxoglutarate dehydrogenase E1 component	1.7 ± 0.1	3.7 ± 0.4	2.2	<0.01	3.3 ± 0.2	2.4 ± 0.1	0.73	<0.01
5517	glucose−6−phosphate isomerase (pgi)	1.0 ± 0.0	3.9 ± 0.1	3.8	<0.01	1.8 ± 0.2	1.2 ± 0.1	0.68	<0.01
5759	thiosulfate sulfurtransferase (cysA−1)	1.5 ± 0.2	3.2 ± 0.5	2.2	<0.01	3.4 ± 0.3	2.0 ± 0.2	0.60	<0.01
6148	cyclic nucleotide−binding domain protein	1.3 ± 0.1	2.6 ± 0.4	2.0	<0.01	3.5 ± 1.0	1.3 ± 0.1	0.39	0.02
6346	catalase/peroxidase HPI (katG)	2.2 ± 0.1	0.8 ± 0.3	0.35	<0.01	1.0 ± 0.3	0.4 ± 0.1	0.39	<0.01
6390	superoxide dismutase (mn)	1.4 ± 0.2	2.9 ± 0.3	2.1	<0.01	1.9 ± 0.2	1.2 ± 0.2	0.61	<0.01
6392	conserved hypothetical protein	3.0 ± 0.2	7.4 ± 0.9	2.5	<0.01	3.6 ± 0.5	2.9 ± 0.4	0.82	<0.01
6855	ribosomal protein L9 (rplI)	1.2 ± 0.1	2.8 ± 0.7	2.4	<0.01	3.0 ± 0.0	1.6 ± 0.2	0.52	<0.01

[a] The prefix of "MSMEG" was omitted from the locus names. HiFe, high iron. LoFe, low iron. $R_{pH} = (S/D)_{pH5}/(S/D)_{pH7}$. $R_{Iron} = (S/D)_{LoFe}/(S/D)_{HiFe}$. p, two-tailed t-test probability for $(S/D)_{pH7}$ versus $(S/D)_{pH5}$ or $(S/D)_{HiFe}$ versus $(S/D)_{LoFe}$.

Table 4. Pearson's Correlation Coefficients of S/D among the Four Culture Cells, Calculated for the 31 Proteins Shown in Table 3

	shocked (pH 5)	control (high iron)	starved (low iron)
control (pH 7)	0.67	0.58	0.64
shocked (pH 5)	1	0.70	0.77
control (high iron)	–	1	0.87

resistant *M. tuberculosis* strain lacking KatG.[32] Many pathogenic bacteria have Tpxs,[33] indicating their roles as possible virulence factors. But the exact biological function of the *M. tuberculosis* Tpx is still unknown.[34] Based on functional and structural characterization, Rho et al. suggested that the *M. tuberculosis* Tpx may play a key role in protecting *M. tuberculosis* against oxidoreductase and being important in the pathogenesis of this organism.[34] Our finding that protein turnover of Tpx was reduced in the *M. smegmatis* cells under low-iron and low-pH conditions indicates that iron limitation and acidification are useful host weaponry against *M. tuberculosis* infection.

In a separate study in which we compared the protein relative abundance of pH 5 versus pH 7 grown *M. smegmatis* cells, we found that KatG (MSMEG6346), AtpD (MSMEG4921), Tpx (MSMEG3484), and Mn (MSMEG6390) had fold change of 0.53, 0.23, 0.72, and 0.65, respectively, all with p <0.0001 (Roxas and Li, unpublished data). In the microarray study by Schnappinger et al. comparing the intraphagosomal *M. tuberculosis* transcriptome profiles with that of an in vitro culture, *katG, atpD*, *tpx*, and *sodA* showed a general trend of suppression upon entering activated macrophages.[35] At 24 h after infection, *katG, atpD*, *tpx*, and *sodA* had fold change of 0.8 ± 0.1, 0.3 ± 0.0, 0.7 ± 0.1, and 0.6 ± 0.1, respectively as measured by amplicon microarrays. In our protein turnover experiments, the turnover for KatG, AtpD, Tpx, and Mn decreased in the low-iron *M. smegmatis* culture cells. KatG, AtpD, and Tpx had lower protein turnover in the acid shocked *M. smegmatis* cells. Although the protein turnover of Mn was accelerated in the acid shocked cells, we cannot rule out that the level of Mn could be reduced as a result of accelerated degradation. Overall, these indicate that the results we obtained for protein turnover in *M. smegmatis* under acid shock and iron starvation are consistent with studies measuring stress response of myco-

(32) Sherman, D. R.; Mdluli, K.; Hickey, M. J.; Arain, T. M.; Morris, S. L.; Barry, C. E., 3rd; Stover, C. K. *Science* **1996**, *272*, 1641−1643.
(33) Wan, X. Y.; Zhou, Y.; Yan, Z. Y.; Wang, H. L.; Hou, Y. D.; Jin, D. Y. *FEBS Lett.* **1997**, *407*, 32−36.
(34) Rho, B. S.; Hung, L. W.; Holton, J. M.; Vigil, D.; Kim, S. I.; Park, M. S.; Terwilliger, T. C.; Pedelacq, J. D. *J. Mol. Biol.* **2006**, *361*, 850−863.
(35) Schnappinger, D.; Ehrt, S.; Voskuil, M. I.; Liu, Y.; Mangan, J. A.; Monahan, I. M.; Dolganov, G.; Efron, B.; Butcher, P. D.; Nathan, C.; Schoolnik, G. K. *J. Exp. Med.* **2003**, *198*, 693−704.

bacteria by other approaches. The approach we demonstrate here provides information about protein dynamics of a living cell. In our ongoing work, we will further improve this approach so that both protein turnover and protein relative abundance can be simultaneously determined from the same culture samples.

CONCLUSION

Using high-capacity instrumentation such as the LTQ-FT mass spectrometer and data processing tools with statistical analysis, we have demonstrated the possibility of automated protein turnover measurements for studying cell stress response on a large scale. Although we only analyzed 151 proteins in this study, the demonstrated procedure is highly similar to that used in large-scale differential abundance measurements[10−12] and thus amendable to automated protein turnover studies at a systems level. We anticipate that the combination of protein turnover and abundance measurements at a systems level will provide new insight into the action mechanisms of antimicrobial agents. Compared to a relative abundance measurement alone, a protein turnover measurement further distinguishes the proteins that are truly down-regulated in de novo synthesis from those that are actively synthesized but also rapidly degraded. Thus, an automated protein turnover measurement on a large scale will afford additional dynamic information for a proteome under various stress conditions. Such information will be useful for intelligent drug design and will probably help accelerate development of more effective drugs against dormant *M. tuberculosis*.

SUPPORTING INFORMATION AVAILABLE

Additional information as noted in text. This material is available free of charge via the Internet at http://pubs.acs.org.

Received for review August 8, 2007. Accepted October 24, 2007.

AC701690D